Lepton Flavor Violation: Constraints from exotic muon to electron conversion [1]

T.S. Kosmas [a] and Sergey Kovalenko [b,2]

[a] *Division of Theoretical Physics, University of Ioannina GR-45110 Ioannina, Greece*

[b] *Departamento de Física, Universidad Técnica Federico Santa María, Casilla 110-V, Valparaíso, Chile*

Abstract

The exotic neutrinoless $\mu^- - e^-$ nuclear conversion is studied within the conventional extensions of the standard model as well as in the minimal supersymmetric (SUSY) models with and without R-parity conservation. The dependence of the $\mu - e$ conversion rates on the nucleon and nuclear structure is consistently taken into account. Using our calculated transition matrix elements and the available experimental data on the branching ratio $R_{\mu e^-}$ for ^{48}Ti and ^{208}Pb as well as the expected experimental sensitivity for ^{27}Al employed as a target in the planned at Brookhaven $\mu^- - e^-$ conversion (MECO) experiment, we extract very severe constraints for the flavor violation parameters. We especially emphasize on the constraints resulting for SUSY R-parity violating parameters.

[1] Based on the Invited talk given by T.S. Kosmas at the *International Conference on Non-Accelerator New Physics(NANP'99)*, Dubna, Russia, 1999.

[2] On leave from the Joint Institut for Nuclear Research, Dubna, Russia.

1 Introduction

The lepton flavor violating (LFV) neutrinoless conversion of a bound 1s-muon to electron in the field of a nucleus [1]-[4]

$$(A, Z) + \mu_b^- \rightarrow e^- + (A, Z)^*, \tag{1}$$

is known as one of the best probes to search for the hypothetical muon and electron flavor non-conservation [1]. So far, the experiments [5]-[8] seeking for $\mu - e$ conversion events have only succeeded to put upper bounds on the branching ratio

$$R_{\mu e^-} = \Gamma(\mu^- \rightarrow e^-)/\Gamma(\mu^- \rightarrow \nu_\mu), \tag{2}$$

i.e. the ratio of the muon-electron conversion rate relative to the total rate of the ordinary muon capture. The best upper limits have been extracted at PSI by the SINDRUM II experiments in the values (at 90% confidence level)

$$R_{\mu e^-} < 7.0 \times 10^{-13} \quad \text{for } ^{48}\text{Ti target [5]}, \tag{3}$$

$$R_{\mu e^-} < 4.6 \times 10^{-11} \quad \text{for } ^{208}\text{Pb target [6]}. \tag{4}$$

These limits are improvements over the previous limits set at TRIUMF [7] a decade ago using the same targets.

At present, two $\mu - e$ conversion experiments are launched, the ongoing experiment at PSI using ^{48}Ti target [5], and the planned MECO experiment at Brookhaven [8] using ^{27}Al target. The expected sensitivity on $R_{\mu e^-}$ in the PSI experiment is 10^{-14} while in the Brookhaven experiment it will be roughly

$$R_{\mu e^-} < 2 \times 10^{-17} \quad \text{for}^{27}\text{Al target [8]}, \tag{5}$$

which implies an improvement over the existing limits by about four orders of magnitude.

The MECO experiment is going to be conducted in a new μ beam line at the AGS, where the muons are produced using a pulsed proton beam [3]. The proton energy will be chosen in the range of 8-20 GeV to optimize the μ^- flux per unit time. Furthermore, the number of electrons with energy $E_e = 104$ MeV, equal to the energy for the coherent peak in ^{27}Al, is very much suppressed. This is in contrast with the case of $\mu^- \rightarrow e^-\gamma$, where the electron flux from $\mu^- \rightarrow e^-\nu\bar{\nu}$ decay is peaked at the energy of the electrons from $\mu^- \rightarrow e^-\gamma$.

For such experiments the knowledge of nuclear transition matrix elements for all accessible $\mu^- \rightarrow e^-$ channels of the targets employed are of significant importance [9]-[13]. In this work we use the transition matrix elements calculated for the aforementioned isotopes in the coherent mode to constrain the lepton flavor violating parameters of various Lagrangians predicting this exotic process (e.g. scalar and vector couplings, neutrino mixing angles and masses [11]-[14], supersymmetric R-parity violating couplings [15]-[17] etc.). To this aim the recent experimental data and the expected sensitivity of the MECO experiment.

As is well known, only the coherent rate can be measured because it is free from background events from bound muon decay and radiative muon capture followed by a fully asymmetric e^+e^- pair creation [8]. On the other hand, previous studies of $\mu - e$ conversion

rates [10]-[12] have shown that for all mechanisms the coherent mode dominates the process (1) which means that this is the most important channel. The incoherent reaction leading to excited nuclear states is suppressed due to Pauli blocking effects and it is much harder to calculate but its knowledge is also useful in order to determine the experimentally interesting quantity of the ratio of the coherent to the total $\mu^- - e^-$ rate (see Refs. [9]-[13]).

2 $\mu^- - e^-$ conversion within common extensions of Standard Model

The family quantum numbers L_e, L_μ, L_τ are conserved within the standard model (SM) in all orders of perturbation theory. However this is an accidental consequence of the SM field content and gauge invariance. Physics beyond the SM can easily spoil this property. Processes like $\mu - e$ conversion, which is forbidden in the standard model by muon and electron quantum number conservation, play an important role in the study of flavor changing neutral currents and possible physics beyond the SM.

On the particle physics side [1, 2], there are many mechanisms of the $\mu - e$ conversion constructed in the literature (see [15]-[17] and references therein). All these mechanisms fall into two different categories: photonic and non-photonic. Mechanisms from different classes significantly differ from the point of view of the nucleon and nuclear structure calculations. This stems from the fact that they proceed at different distances and, therefore, involve different details of the structure.

The long-distance photonic mechanisms are mediated by the photon exchange between the quark and the $\mu - e$-lepton currents. These mechanisms resort to the lepton-flavor non-diagonal electromagnetic vertex which is presumably induced by the non-standard model physics at the loop-level. The $\mu - e$ lepton-flavor violating loop can appear as the $\nu - W$ loop [Fig.1(a)] with the massive neutrinos ν_i and the loop with the supersymmetric particles such as the neutralino(chargino)-slepton(sneutrino) [Fig.1(d)]. In the R-parity violating SUSY models there are also lepton-slepton and quark-squark loops generated by the superpotential couplings λLLE^c and $\lambda' LQD^c$ respectively.

The short-distance non-photonic mechanisms contain heavy particles in intermediate states and can be realized at tree level [Fig.2], at 1-loop-level [Fig.1(a,b,d,e)] or at the level of box diagrams [Fig.1(c)]. The tree-level diagrams can be constructed in the R-parity violating SUSY models with the virtual Z-boson, squarks $\tilde{u}, \tilde{d}$ and sneutrinos $\tilde{\nu}_i$ [Fig.2]. The 1-loop diagrams of the non-photonic mechanisms include the diagrams similar to those for the photonic mechanisms but with the Z-boson instead of the photon [Fig.1(a,d)] as well as additional Z-boson couplings to the neutrinos and neutralinos [Fig.1(b,e)]. The box diagrams are constructed of the W-bosons and massive neutrinos [Fig.1(c)] as well as similar boxes with neutralinos and sleptons or charginos and sneutrinos.

Our purpose is to calculate the contribution of the above-described mechanisms to the $\mu^- - e^-$ conversion branching ratio (2). At the first step we construct the effective $\mu^- - e^-$ conversion Hamiltonian for these mechanisms in terms of nucleon degrees of freedom of a nucleus involved in the process. This will allow us to accomplish the calculation of $R_{\mu e^-}$ by applying the conventional nuclear structure methods using non-relativistic impulse

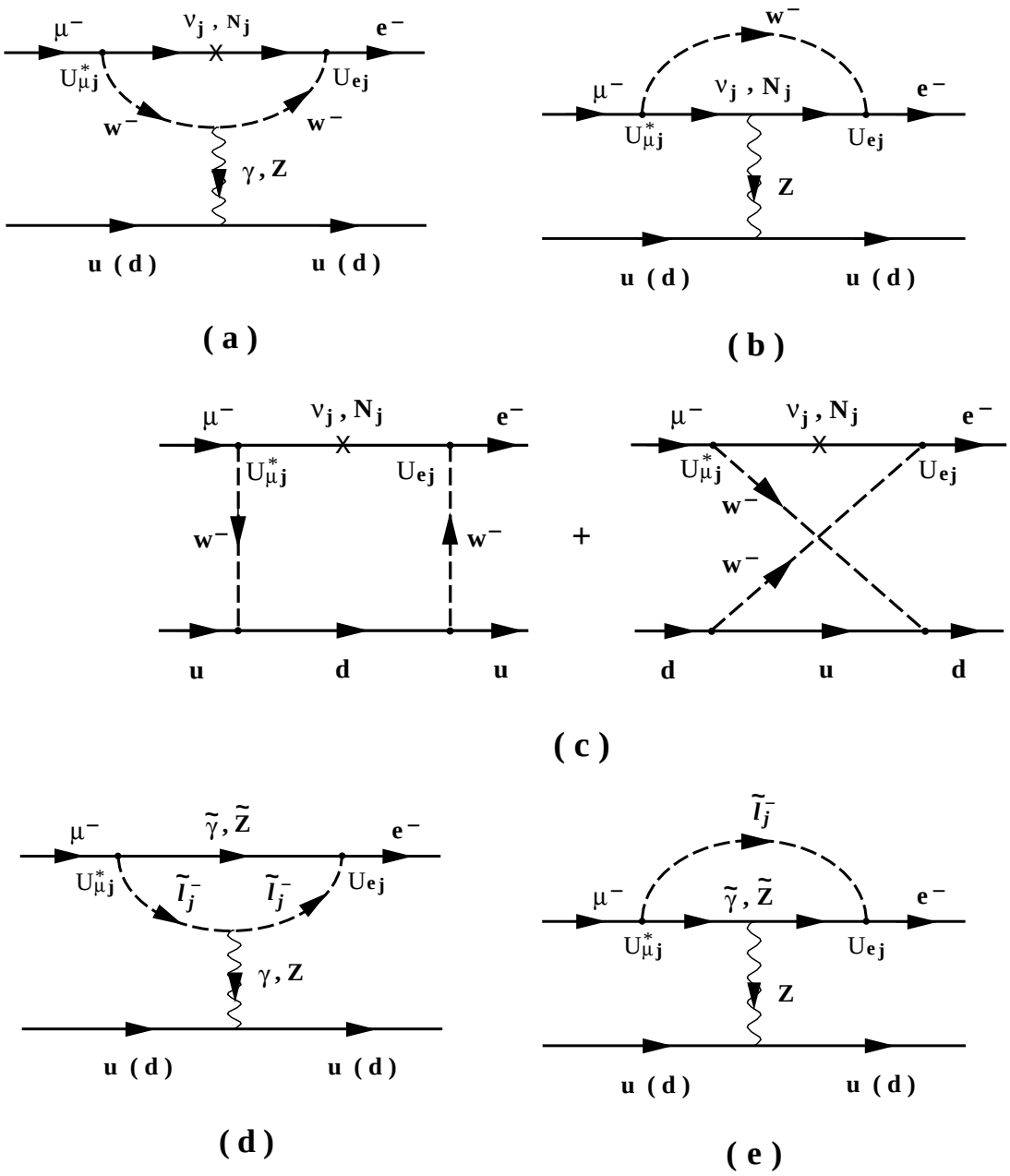

Figure 1: Photonic and non-photonic mechanisms exhibiting the $\mu^- - e^-$ process within the context of conventional extensions of the standard model (a-c), as well as supersymmetric theories (d,e) with R-parity conservation. The hadronic vertex is mediated by photon exchange (a,d), Z-particle exchange (a,b,d,e), and W-boson exchange (c).

approximation.

For the photonic diagrams of Fig. 1(a,d) the hadronic vertex represents the usual nucleon electromagnetic current

$$J_\lambda^{(1)} = \bar{N}_p \gamma_\lambda N_p \;=\; \bar{N} \gamma_\lambda \frac{1}{2} \left(1 + \tau_3\right) N \qquad (photonic) \tag{6}$$

N is the nucleon isospin doublet $N^T = (N_p, N_n)$ with N_p, N_n being the proton and neutron spinors.

In the case of the non-photonic mechanisms of Fig. 1 the hadronic currents are either the SM neutral currents coupled to Z-boson [Fig. 1(a,b,d,e)] or the effective currents derived

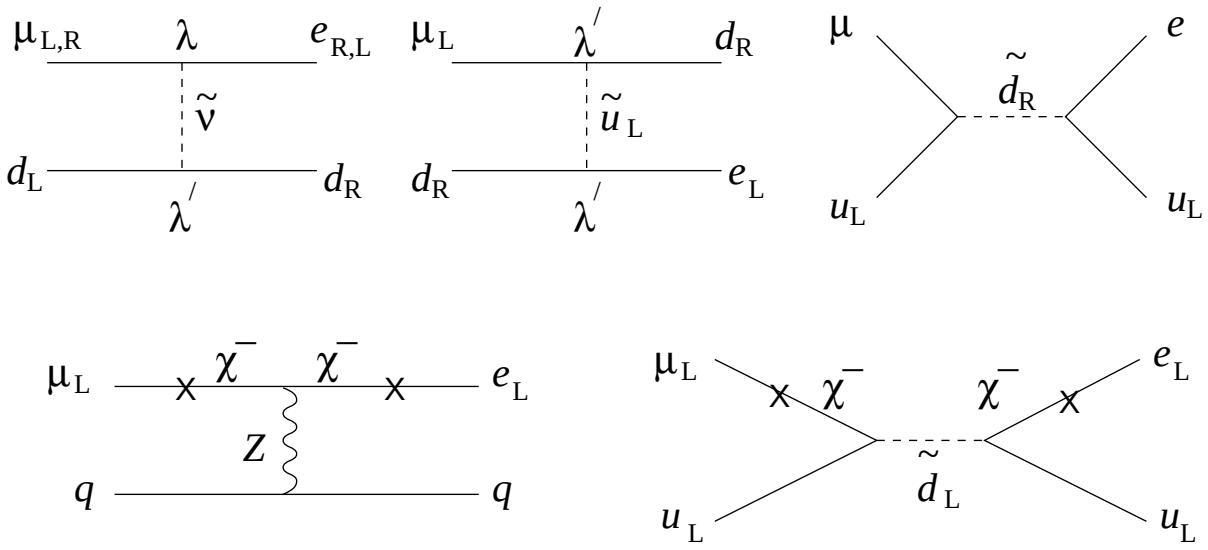

Figure 2: Leading $\not{R}_p$ MSSM diagrams contributing to $\mu - e$ conversion at tree-level. The chargino-lepton mixing is schematically denoted by crosses (X) on the lepton lines.

after an appropriate Fierz transformation from the effective operators of the box diagrams [Fig. 1(c)] involving heavy particles. These currents can be written in terms of the nucleon doublet field as

$$J_\lambda^{(2)} = \bar{N}\gamma_\lambda \frac{1}{2}\left[(3 + f_V\beta\tau_3) - (f_V\beta'' + f_A\beta'\tau_3)\gamma_5\right] N \qquad (non - photonic) \tag{7}$$

where f_V, f_A represent the vector, axial vector static nucleon form factors ($f_A/f_V = 1.24$) and the parameters β, β', β'', for the models adopted take the values given in Ref. [11]. The parameter β is defined as $\beta = \beta_1/\beta_0$, with β_0 (β_1) the isoscalar (isovector) couplings at the quark level. We should note that, in general, the parameters β, β' and β'' are functions of $sin^2\theta_W$. For example, in the case of Z-exchange we have $\beta' = 3/2sin^2\theta_W = 6.90$.

The corresponding leptonic currents for the photonic and non-photonic mechanism of Figs. 1 are given in Ref. [11].

In the minimal SUSY model with a most general form of R-parity violation (for review see, for instance, [18]) all the possible tree-level diagrams for the $\mu^- - e^-$ conversion process are shown in Fig. 2 [15],[17]. To write down the low-energy $\mu - e$ conversion Lagrangian at quark level one starts from the well known R-parity violating superpotential and integrates out heavy intermediate fields. For the diagrams of Fig. 2 the corresponding 4-fermion low-energy effective Lagrangian at the quark level takes the form [17] (first order of perturbation theory)

$$\begin{aligned}\mathcal{L}_{eff}^q &= \frac{G_F}{\sqrt{2}} j_\mu \left[\eta_L^{ui} J_{uL(i)}^\mu + \eta_R^{ui} J_{uR(i)}^\mu + \eta_L^{di} J_{dL(i)}^\mu + \eta_R^{di} J_{dR(i)}^\mu\right] \\ &+ \frac{G_F}{\sqrt{2}} \left[\bar{\eta}_R^{di} J_{dR(i)} j_L + \bar{\eta}_L^{di} J_{dL(i)} j_R\right]. \end{aligned} \tag{8}$$

(i runs over generations so that $q_i = u_i, d_i$ with $u_i = u, c, t$ and $d_i = d, s, b$) where the coefficients η_k^q contain the $\not{R}_p$ SUSY parameters [17]. The color singlet currents $J_{q_{L/R}(i)}^\mu$ and $J_{d_{L/R}(i)}$ at the quark level are written as

$$J_{q_{L/R}(i)}^\mu = \bar{q}_i \gamma^\mu P_{_{L/R}} q_i, \qquad J_{d_{L/R}(i)} = \bar{d}_i P_{_{L/R}} d_i.$$

where $P_{_{L,R}} = (1 \mp \gamma_5)/2$. The leptonic currents are written as

$$j^\mu = \bar{e}\gamma^\mu P_{_L}\mu, \qquad j_{_{L/R}} = \bar{e}P_{_{L/R}}\mu$$

At the next step we rewrite Eq. (8), specified at the quark level, in terms of the nucleon degrees of freedom. This is usually achieved by utilizing the on-mass-shell matching condition [19] and gives

$$\mathcal{L}^N_{eff} = \frac{G_F}{\sqrt{2}}\left[\bar{e}\gamma_\mu(1-\gamma_5)\mu \cdot J^\mu + \bar{e}\mu \cdot J_+ + \bar{e}\gamma_5\mu \cdot J_-\right]. \tag{9}$$

where now the hadronic (nucleon) currents are

$$\begin{aligned} J^\mu &= \bar{N}\gamma^\mu\left[(\alpha_V^{(0)} + \alpha_V^{(3)}\tau_3) + (\alpha_A^{(0)} + \alpha_A^{(3)}\tau_3)\gamma_5\right] N, \\ J^\pm &= \bar{N}\ \left[(\alpha_{\pm S}^{(0)} + \alpha_{\pm S}^{(3)}\tau_3) + (\alpha_{\pm P}^{(0)} + \alpha_{\pm P}^{(3)}\tau_3)\gamma_5\right] N, \end{aligned} \tag{10}$$

The coefficients $\alpha_K^{(0,3)}$, with $K = S, V, A, P$, in Eq. (10) include the nucleon form factors (functions of the momentum transfer $\mathbf{q}^2$) for scalar, vector, axial vector and pseudoscalar contributions, respectively (for their definition see Ref. [17]). Since, however, the maximum momentum transfer $\mathbf{q}^2$ in $\mu - e$ conversion is much smaller than the typical scale of nucleon structure ($|\mathbf{q}| \approx m_\mu/c$, with $m_\mu = 105.6MeV$, the muon mass), we can safely neglect the $\mathbf{q}^2$-dependence of the nucleon form factors.

3 Nucleon and nuclear structure dependence of the $\mu^- - e^-$ conversion branching ratio

One of the most interesting quantities in $\mu^- - e^-$ conversion, both from theoretical and experimental points of view, is the branching ratio $R_{\mu e^-}$ defined in Eq. (2). The expression which gives $R_{\mu e^-}$ in the case of the dominant coherent channel has been written as [9]

$$R_{\mu e^-} = \rho\gamma, \tag{11}$$

where ρ is nearly independent of nuclear physics [11] and contains the flavor-violating parameters mentioned before. Thus, e.g. for photon-exchange ρ is given by

$$\rho = (4\pi\alpha)^2\frac{|f_{M1} + f_{E0}|^2 + |f_{E1} + f_{M0}|^2}{(G_F m_\mu^2)^2} \tag{12}$$

This expression contains the electromagnetic form factors f_{E0}, f_{E1}, f_{M0}, f_{M1} parametrized in a specific elementary model [11].

The function $\gamma(A, Z)$ of Eq. (11) includes about all the nuclear information. By assuming that the total rate of the ordinary muon capture rate is described by the Goulard-Primakoff function f_{GP}, $\gamma(A, Z)$ is defined as

$$\gamma(A, Z) \equiv \gamma = \frac{E_e p_e}{m_\mu^2}\frac{M^2}{G^2 Z f_{GP}(A, Z)}, \tag{13}$$

where $G^2 \approx 6$. Thus, the nuclear aspects of the $\mu^- \to e^-$ branching ratio $R_{\mu e^-}$ are mainly included in the matrix elements M^2 [4], which in the proton-neutron representation, are written as

$$M^2 = (M_p + M_n)^2 \tag{14}$$

In general, the transition matrix elements $\mathcal{M}_{p,n}$ in Eq. (14) depend on the final nuclear state populated during the $\mu - e$ conversion. For ground state to ground state transitions ($gs \to gs$) in spherically symmetric nuclei the following integral representation is valid

$$\mathcal{M}_{p,n} = 4\pi \int j_0(p_e r)\Phi_\mu(r)\rho_{p,n}(r)r^2 dr \tag{15}$$

where $j_0(x)$ the zero order spherical Bessel function and $\rho_{p,n}$ the proton (p), neutron (n) nuclear density normalized to the atomic number Z and neutron number N of the participating nucleus, respectively. The space dependent part of the muon wave function $\Phi_\mu(\mathbf{r})$, a spherically symmetric function, can be obtained by solving numerically the Schrödinger and Dirac equations with the Coulomb potential.

For the coherent rate in light nuclei the factorization approximation (see Ref. [10]) is very good and $M^2_{\rm coh}$ can be expressed in terms of the nuclear form factors $F_Z(q^2)$ (for protons) and $F_N(q^2)$ (for neutrons) which are easily estimated (for this channel only the ground state wave function of the studied nucleus is required). These form factors are defined as

$$F_Z = \frac{1}{Z}\sum_j \hat{j}(j\|j_0(qr)\|j)\left(V_j^p\right)^2, \tag{16}$$

$$F_N = \frac{1}{N}\sum_j \hat{j}(j\|j_0(qr)\|j)\left(V_j^n\right)^2, \tag{17}$$

and contain the single-particle orbit occupancies $(V_j)^2$ for the evaluation of which one must use a nuclear model in the proton-neutron representation, e.g. QRPA (for ^{48}Ti and ^{208}Pb see Ref. [11]), shell-model (for ^{27}Al see Ref. [20]) etc.

By using the Lagrangian (9) one can deduce a similar expression to that of Eq. (11) for the $\mu - e$ conversion branching ratio as

$$R_{\mu e^-} = \frac{G_F^2}{2\pi}\ \frac{p_e E_e\ (\mathcal{M}_p + \mathcal{M}_n)^2}{G^2\ Z f_{GP}(A,Z)}\ \ \mathcal{Q} \tag{18}$$

where

$$\begin{aligned}\mathcal{Q} \ =\ & 2|\alpha_V^{(0)} + \alpha_V^{(3)}\ \phi|^2 + |\alpha_{+S}^{(0)} + \alpha_{+S}^{(3)}\ \phi|^2 + |\alpha_{-S}^{(0)} + \alpha_{-S}^{(3)}\ \phi|^2 \\ & +2\ \mathrm{Re}\{(\alpha_V^{(0)} + \alpha_V^{(3)}\ \phi)[\alpha_{+S}^{(0)} + \alpha_{-S}^{(0)} + (\alpha_{+S}^{(3)} + \alpha_{-S}^{(3)})\ \phi]\}\end{aligned} \tag{19}$$

with

$$\phi = (\mathcal{M}_p - \mathcal{M}_n)/(\mathcal{M}_p + \mathcal{M}_n) \tag{20}$$

The quantity $\mathcal{Q}$ in Eq. (19) depends weakly on the nuclear parameters determining the factor ϕ. In fact, the terms depending on ϕ are small and in practice the nuclear dependence of $\mathcal{Q}$ can be neglected. Thus, the corresponding upper bounds on $\mathcal{Q}$ determine the sensitivity

to the $\not{R}_p$ SUSY signals arriving at the detector in various $\mu - e$ conversion experiments (see results below).

A usual approximate expression for the ratio ϕ of Eq. (20), containing the nuclear parameters A, the atomic weight, and Z the total charge of the nucleus, is the following

$$\phi \approx \tilde{\phi} = (A - 2Z)/A, \tag{21}$$

The latter equation can be obtained assuming that $M_p \approx Z\ F_Z \langle \Phi \rangle$ and $M_n \approx N\ F_N \langle \Phi \rangle$ where $\langle \Phi \rangle$ represents the mean value of the muon wave function $\Phi_\mu(r)$. For light and medium nuclei $F_Z \approx\ F_N$ and Eq. (21) is a good approximation. For isoscalar nuclei, i.e. $A = 2Z$, $\phi \approx \tilde{\phi} = 0$ (see Sect. 4).

4 Results and Discussion.

The pure nuclear physics calculations needed for the $\mu - e$ conversion studies involve mainly the integrals of Eq. (15). For the currently interesting nuclei Al, Ti and Pb the results for M_p and M_n are shown in Table 1. They have been calculated using proton densities ρ_p from the electron scattering data [21] and neutron densities ρ_n from the analysis of pionic atom data [22]. We have employed an analytical form for the muon wave function obtained by solving the Schrödinger equation using the Coulomb potential produced by the charge densities discussed before. In this way the nucleon finite size was taken into consideration. Moreover, we included vacuum polarization corrections as in Ref. [12].

In solving the Schrödinger equation we have used modern neural networks techniques [23] which give the wave function $\Phi_\mu(r)$ in the analytic form of a sum over sigmoid functions. Thus, in Eq. (15) only a simple numerical integration is finally required. To estimate the influence of the non-relativistic approximation on the muon wave function $\Phi_\mu(\mathbf{r})$, we have also determined it by solving the Dirac equation. The results do not significantly differ from those of the Schrödinger picture.

In Table 1 we also show the muon binding energy ϵ_b (obtained as output of the Dirac and Schrödinger solution) and the experimental values for the total rate of the ordinary muon capture $\Gamma_{\mu c}$ taken from Ref. [24].

Using values for M_p and M_n for a set of nuclei throughout the periodic table [12] one can estimate the nuclear structure dependence of the quantities ρ and $\mathcal{Q}$. In Table 2 we show the results obtained for the ratio ϕ of Eq. (20) and its approximate expression $\tilde{\phi}$ of Eq. (21). We see that ϕ is very small ($-0.17 \leq \phi \leq 0.04$) and, because the terms of the quantity $\mathcal{Q}$ depending on ϕ are also small, we conclude that the nuclear dependence of $\mathcal{Q}$ can be ignored as we have discussed in Sect. 2.

Since there is at maximum $\approx 15\%$ difference between ϕ and $\tilde{\phi}$ and because the isovector terms of the quantity $\mathcal{Q}$ are small, especially for light nuclear systems, one can also use $\tilde{\phi}$ in the expression (A,Z) dependence of $\mathcal{Q}$.

The results of Table 1 can be exploited for setting constraints on the parameters of a specific gauge model predicting the $\mu - e$ process. In Table 3 we quote the upper bounds for the quantities ρ and $\mathcal{Q}$ derived by using the recent experimental data on the branching ratio $R_{\mu e^-}$ given in Eqs. (3), (4) and the expected experimental sensitivity of the Brookhaven

experiment, $R_{\mu e^-} < 2 \times 10^{-17}$ [see Eq. (5)]. The limits of ρ and $\mathcal{Q}$ quoted in Table 3 are improvements by about four orders of magnitude over the previous ones.

We should stress that the limits on the quantities ρ of Eq. (12) and $\mathcal{Q}$ of Eqs. (19), are the only constraints imposed by the $\mu - e$ conversion on its underlying elementary particle physics. One can extract upper limits on the individual lepton flavor violation parameters (couplings of scalar, vector currents, neutrino masses etc. [1, 4, 11, 17]) under certain assumptions like the commonly assumed dominance of only one component of the $\mu - e$ conversion Lagrangian which is equivalent to constrain one parameter or product of the parameters at a time. For example, in the case of $\not{R}_p$ SUSY mechanisms, in order to learn about the size and the regularities of possible violation of R-parity, one needs some information on the parameters λ, λ', μ_i and the sneutrino vacuum expectation values $\langle \tilde{\nu}_i \rangle$ [25]. Using the upper limits for $\mathcal{Q}$ given in Table 3 we can derive under the above assumptions the constraints on $\alpha_K^{(\tau)}$ of Eq. (19) and the products of various $\not{R}_p$ parameters. Thus, the bounds obtained for the scalar current couplings $\alpha_{\pm S}^{(0)}$ in the R-parity violating Lagrangian for the ^{27}Al target [20, 26] are $|\alpha_{\pm S}^{(0)}| < 7 \times 10^{-10}$. The limit for $\alpha_{\pm S}^{(0)}$ obtained with the data of Ti target [5] is $|\alpha_{\pm S}^{(0)}| < 1.1 \times 10^{-7}$, i.e. more than two orders of magnitude weaker than the limit of ^{27}Al.

With these limits it is straightforward to derive constraints on the parameters of the initial LFV Lagrangian. In Table 4 we list the most stringent constraints on the products of the trilinear $\not{R}_p$ couplings which we obtained from the experimental limit on $\mu - e$ conversion in ^{48}Ti [see Eq. (3)] and from the expected experimental sensitivity of MECO detector using ^{27}Al as a target material [see Eq. (5)]. The corresponding constraints for ^{208}Pb are significantly weaker and they are not presented in Table 4. In this table B denotes a scaling factor defined as

$$B = (R_{\mu e}^{exp}/7.0 \cdot 10^{-13})^{1/2},$$

which can be used for reconstructing the limits for the other experimental upper limits on the branching ratio $R_{\mu e}^{exp}$. As seen from Table 4, the $\mu - e$-conversion limits on the products $\lambda\lambda'$ are significantly more stringent than those previously known in the literature [18] and given in the 2nd column. In Refs. [16, 17] it was shown that except few cases, the constraints on $\lambda'\lambda'$, $\lambda\lambda'$ and $\lambda\lambda$ obtained from $\mu - e$ conversion data are better than those derived from any other process.

As we have mentioned at the beginning, significantly better improvement on these limits is expected from the ongoing experiments at PSI [5] and even better from the MECO experiment at Brookhaven [8]. This would make the $\mu - e$ conversion constraints better than those from the other processes in all the cases.

Before closing we should note that the last four limits for $\lambda'\lambda$ in Table 4 originate from the contribution of the strange nucleon sea. These limits are comparable to the other $\mu - e$ constraints derived from the valence quarks contributions.

5 Summary and Conclusions.

The transition matrix elements of the flavor violating $\mu^- - e^-$ conversion are of notable importance in computing accurately the corresponding rates for each accessible channel of

this exotic process. Such calculations provide useful nuclear-physics inputs for the expected new data from the PSI and MECO experiments to put more severe bounds on the muon-number-changing parameters (isoscalar couplings, etc.) determining the effective currents in various models that predict the exotic $\mu^- - e^-$ process.

In the case of the R-parity violating interactions discussed here we have studied all the possible tree-level contributions to the $\mu - e$ conversion in nuclei taking into account the nucleon and nuclear structure effects. We found new important contribution to $\mu^- \to e^-$ originating from the strange quark sea in the nucleon which is comparable with the usual contribution of the valence u, d quarks.

From the existing data on $R_{\mu e^-}$ in ^{48}Ti and ^{208}Pb and the expected sensitivity of the designed MECO experiment [8] we obtained stringent upper limits on the quantities ρ and $\mathcal{Q}$ introduced in Eqs. (12) and (19). They can be considered as theoretical sensitivities of a particular experiment to the $\mu^- - e^-$ conversion signals for various targets employed. Thus, these quantities are helpful for comparing different $\mu - e$ conversion experiments. We also extracted the upper limits on the products of the trilinear $\not{R}_p$parameters of the type $\lambda\lambda'$ which are significantly more severe than those existing in the literature. As to the other products, the following observation was formulated in Refs. [16, 17]. If the ongoing experiments at PSI [5] and Brookhaven [8] will have reached the quoted sensitivities in the branching ratio $R_{\mu e^-}$ then the $\mu - e$ constraints on all the products of the $\not{R}_p$ parameters $\lambda\lambda$, $\lambda'\lambda$, $\lambda'\lambda'$ measurable in $\mu - e$ conversion will become more stringent than those from any other processes. This is especially important in view of the fact that no comparable improvements of the other experiments testing these couplings are expected in the near future.

T.S.K would like to acknowledge partial support of this work by Ioannina University grants and the NANP-99 Conference Organizers for hospitality at Dubna.

References

[1] W.J. Marciano and A.I. Sanda, Phys. Rev. Lett. **38**, 1512 (1977); Phys. Lett. **B 67**, 303 (1977).

[2] J.D. Vergados, Phys. Reports **133**, 1 (1986).

[3] W. Molzon, The improved tests of muon and electron flavor symmetry in muon processes, Spring. Trac. Mod. Phys., in press.

[4] T.S. Kosmas, G.K. Leontaris and J.D. Vergados, Prog. Part. Nucl. Phys. **33**, 397 (1994).

[5] C. Dohmen *et al.*, (SINDRUM II Collaboration), Phys. Lett. **B 317** (1993) 631; H.K. Walter, Phys. Atom. Nucl. **61** (1998) 1253.

[6] W. Honecker *et al.*, (SINDRUM II Collaboration), Phys. Rev. Lett. **76** (1996) 200.

[7] S. Ahmad *et al.*, (TRIUMF Collaboration), Phys. Rev. Lett. **59** (1987) 970.

[8] W. Molzon, The MECO Experiment: A search for $\mu^- N \to e^- N$ with sensitivity below 10^{-16}, Invited talk at Int. Conf. on "Symmetries in Physics at Intermediate and High Energies and Applications", Ioannina-Greece, Sept. 30 - Oct. 5, 1998.

[9] T.S. Kosmas and J.D. Vergados, Nucl. Phys. **A 510** (1990) 641.

[10] T.S. Kosmas, J.D. Vergados, and A. Faessler, Phys. Atom. Nucl. **61** (1998) 1161.

[11] T.S. Kosmas, A. Faessler, and J.D. Vergados, J. Phys. **G 23** (1997) 693;

[12] H.C. Chiang, E. Oset, T.S. Kosmas, A. Faessler, and J.D. Vergados, Nucl. Phys. **A 559** (1993) 526.

[13] J. Schwieger, T.S. Kosmas, and A. Faessler, Phys. Lett. **B 443** (1998) 7.

[14] R. Barbieri and L. Hall, Phys. Lett. **B 338** (1994) 212; R. Barbieri, L. Hall, and A. Strumia, Nucl. Phys. **B 445** (1995) 219.

[15] J.E. Kim, P. Ko, and D.-G. Lee, Phys. Rev. **D 56** (1997) 100, hep-ph/9701381.

[16] K. Huitu, J. Maalampi, M. Raidal, and A. Santamaria, Phys. Lett. **B 430** (1998) 355, hep-ph/9712249.

[17] A. Faessler, T.S. Kosmas, S. Kovalenko, and J.D. Vergados, hep-ph/9904335.

[18] G. Bhattacharyya, Nucl. Phys. Proc. Suppl. 52 A (1997) 83, IFUP-TH 43/97, hep-ph/9709395; H. Dreiner, in Proc. of *Perspectives on Supersymmetry*, Ed. by G.L. Kane, World Scientific, 462 (1999); P. Roy, Plenary talk given at the *Pacific Particle Physics Phenomenology Conference*, Seoul, Korea, Oct. 31 - Nov. 2, 1997, hep-ph/9712520; R. Barbier et al. Report of the GDR working group on the R-parity violation, hep-ph/9810232.

[19] A. Faessler, S. Kovalenko, F. Šimkovic, and J. Schwieger, Phys. Rev. Lett. **78** (1997) 183; A. Faessler, S. Kovalenko, F. Simkovic, Phys. Rev. **D 57**, 55004 (1998).

[20] T. Siiskonen, J. Suhonen, and T.S. Kosmas, Phys. Rev. **C 60** (Rapid Communication), 62501 (1999).

[21] H. de Vries, C.W. de Jager and C. de Vries, Atomic Data and Nuclear Data Tables, **36** (1987) 495.

[22] W.R. Gibbs and B.F. Gibson, Ann. Rev. Nucl. Part. Sci. **37** (1987) 411; C. Garcia-Recio, J. Nieves and E. Oset, Nucl. Phys. **A 547** (1992) 473.

[23] I.E. Lagaris, A. Likas, and D.I. Fotiadis, Comp. Phys. Commun. **104** (1997) 1.

[24] T. Suzuki, *et al.*, Phys. Rev. **C 35** (1987) 2212.

[25] V.A. Bednyakov, A. Faessler, and S. Kovalenko, Phys. Lett. **B 442** (1998) 203.

[26] T. Siiskonen, T.S. Kosmas, and J. Suhonen, Phys. Rev. **C** , to be submitted.

Nucleus	$\lvert\mathbf{p}_e\rvert\,(fm^{-1})$	$\epsilon_b\,(MeV)$	$\Gamma_{\mu c}\,(\times 10^6\,s^{-1})$	$\mathcal{M}_p\,(fm^{-3/2})$	$\mathcal{M}_n\,(fm^{-3/2})$
^{27}Al	0.531	-0.470	0.71	0.047	0.045
^{48}Ti	0.529	-1.264	2.60	0.104	0.127
^{208}Pb	0.482	-10.516	13.45	0.414	0.566

Table 1: Transition matrix elements (muon-nucleus overlap integrals $\mathcal{M}_{p,n}$ of Eq. (15)) evaluated by using the exact muon wave function obtained via neural networks techniques. Other useful quantities (see text) are also included.

A	Z	ϕ(A,Z)	$\tilde{\phi}$(A,Z)
12.	6.	0.000	0.000
24.	12.	0.014	0.000
27.	13.	0.000	-0.037
32.	16.	0.023	0.000
40.	20.	0.037	0.000
44.	20.	-0.063	-0.091
48.	22.	-0.083	-0.083
63.	29.	-0.056	-0.079
90.	40.	-0.054	-0.111
112.	48.	-0.108	-0.143
208.	82.	-0.152	-0.212
238.	92.	-0.175	-0.227

Table 2: The variation of the quantities ϕ [see Eq. (20)] and its approximate expression $\tilde{\phi}$ [see Eq. (21)] through the periodic table.

Mechanism	^{27}Al	^{48}Ti	^{208}Pb
Photonic	$\rho \leq 4.6 \times 10^{-18}$	$\rho \leq 8.2 \times 10^{-14}$	$\rho \leq 3.2 \times 10^{-12}$
W-boson exchange	$\rho \leq 5.8 \times 10^{-19}$	$\rho \leq 3.0 \times 10^{-14}$	$\rho \leq 1.1 \times 10^{-12}$
SUSY sleptons	$\rho \leq 1.8 \times 10^{-18}$	$\rho \leq 3.0 \times 10^{-14}$	$\rho \leq 1.1 \times 10^{-12}$
SUSY Z-exchange	$\rho \leq 7.3 \times 10^{-19}$	$\rho \leq 0.7 \times 10^{-14}$	$\rho \leq 0.2 \times 10^{-12}$
$\not{R}_p$ SUSY	$\mathcal{Q} \leq 5.10 \cdot 10^{-19}$	$\mathcal{Q} \leq 1.25 \cdot 10^{-14}$	$\mathcal{Q} \leq 2.27 \cdot 10^{-13}$

Table 3: Upper limits on the elementary particle sector of the exotic $\mu - e$ conversion branching ratio (quantity ρ of Eq. (12) and quantity $\mathcal{Q}$ of Eq. (19)) extracted by using the recent experimental data for the nuclear targets ^{48}Ti and ^{208}Pb [5, 6] and the sensitivity of the MECO experiment for the ^{27}Al target [8].

Parameters	Previous bounds	$^{48}Ti \times B$	$^{27}Al \times B$
$\lvert\lambda'_{211}\,\lambda_{212}\rvert$	$4.5 \cdot 10^{-3}$	$4.1 \cdot 10^{-9}$	$5.5 \cdot 10^{-11}$
$\lvert\lambda'_{311}\,\lambda_{312}\rvert$	$6.0 \cdot 10^{-3}$	$4.1 \cdot 10^{-9}$	$5.5 \cdot 10^{-11}$
$\lvert\lambda'_{111}\,\lambda_{121}\rvert$	$1.5 \cdot 10^{-5}$	$4.1 \cdot 10^{-9}$	$5.5 \cdot 10^{-11}$
$\lvert\lambda'_{311}\,\lambda_{321}\rvert$	$6.0 \cdot 10^{-3}$	$4.1 \cdot 10^{-9}$	$5.5 \cdot 10^{-11}$
$\lvert\lambda'_{222}\,\lambda_{212}\rvert$	$9.0 \cdot 10^{-3}$	$7.7 \cdot 10^{-9}$	$1.0 \cdot 10^{-10}$
$\lvert\lambda'_{322}\,\lambda_{312}\rvert$	$1.2 \cdot 10^{-2}$	$7.7 \cdot 10^{-9}$	$1.0 \cdot 10^{-10}$
$\lvert\lambda'_{122}\,\lambda_{121}\rvert$	$1.0 \cdot 10^{-3}$	$7.7 \cdot 10^{-9}$	$1.0 \cdot 10^{-10}$
$\lvert\lambda'_{322}\,\lambda_{321}\rvert$	$1.2 \cdot 10^{-2}$	$7.7 \cdot 10^{-9}$	$1.0 \cdot 10^{-10}$

Table 4: The upper bounds on the products of the trilinear $\not{R}_p$parameters $\lambda'_{ijk}\lambda_{lmn}$. Previous bounds in the 2nd column are taken from Refs. [16, 18]. The new $\mu^- - e^-$ conversion bounds in the 3rd and the 4th columns are obtained using the SINDRUM II data for ^{48}Ti target [see Eq. (3)] and the expected sensitivity of the MECO target ^{27}Al [see Eq. (5)]. These bounds are given for the scalar superpartner masses $\tilde{m} = 100$ GeV (the scaling factor B is defined in the text).